

2010

Transcritical Carbon Dioxide Microchannel Heat Pump Water Heaters: Part II - System Simulation and Optimization

Christopher Goodman
United Technology Research Center

Brian Fronk
Georgia Institute of Technology

Srinivas Garimella
Georgia Institute of Technology

Follow this and additional works at: <http://docs.lib.purdue.edu/iracc>

Goodman, Christopher; Fronk, Brian; and Garimella, Srinivas, "Transcritical Carbon Dioxide Microchannel Heat Pump Water Heaters: Part II - System Simulation and Optimization" (2010). *International Refrigeration and Air Conditioning Conference*. Paper 1159. <http://docs.lib.purdue.edu/iracc/1159>

This document has been made available through Purdue e-Pubs, a service of the Purdue University Libraries. Please contact epubs@purdue.edu for additional information.

Complete proceedings may be acquired in print and on CD-ROM directly from the Ray W. Herrick Laboratories at <https://engineering.purdue.edu/Herrick/Events/orderlit.html>

Transcritical Carbon Dioxide Microchannel Heat Pump Water Heaters: Part II – System Simulation and Optimization

Christopher Goodman¹, Brian Fronk² and Srinivas Garimella^{2*}

¹United Technologies Research Center (UTRC)
East Hartford, CT, USA

²Georgia Institute of Technology, George W. Woodruff School of Mechanical Engineering,
Atlanta, GA USA
(404)-894-7479; srinivas.garimella@me.gatech.edu

* Corresponding Author

ABSTRACT

This paper presents the development of a transcritical CO₂ heat pump water heating system model incorporating analytical heat exchanger models and an empirical compressor model. This study investigated the effects of a suction line heat exchanger (SLHX) and once-through versus multi-pass water heating schemes. The once-through systems outperformed the multi-pass systems by 10% for the system without a SLHX and 15% with a SLHX. However, a gas cooler twice as large is required. The SLHX was shown to benefit system performance at higher evaporator temperatures with improvements of 16.5% for the once-through and 4% for the multi-pass systems. This study can be used to improve the design of microchannel based transcritical CO₂ heat pumps; evaluate the impact of varying water inlet temperature, desired outlet temperature and evaporation temperature on system performance; and quantify the effect of differential diurnal electricity rates on system operating costs for these different operation schemes.

1. INTRODUCTION

Heat pump water heaters have been shown to be one of the most promising applications of using low global warming potential (GWP) CO₂ as a working fluid (Neksa *et al.*, 1998; Kim *et al.*, 2004). The high temperature lifts required in water heating match well with the temperature glide exhibited by the supercritical CO₂ during heat rejection. The glide allows water delivery temperatures of up to 90°C without significant degradation in system efficiency (2004). Heating water to this temperature with a conventional system (*e. g.*, R134a) can only be done by raising the compressor discharge pressure substantially to avoid temperature pinches. In conventional systems therefore, as the condenser saturation pressure increases, the available enthalpy difference across the vapor-liquid dome decreases, and the compressor pressure ratio increases, drastically reducing system efficiency.

Neksa *et al.* (1998) developed and validated a system model assuming a tube-in-tube gas cooler in a 50 kW system, heating water from 8 to 60°C with a COP that varied from 3.0 to 4.3. Neksa *et al.* (1998) demonstrated a decreasing COP with increasing water temperature at a fixed evaporator pressure. Cecchinato *et al.* (2005) and Rigola *et al.* (2005) each presented comparisons between R134a and CO₂ based heat pump water heaters. Again, each researcher assumed a tube-in-tube gas cooler. Cecchinato *et al.* (2005) showed CO₂ offers improved performance at many operating conditions. However Rigola *et al.* (2005) showed operating at high gas cooler water inlet temperatures can severely degrade CO₂ heat pump performance. Thus, Cecchinato *et al.* (2005) also show that CO₂ systems benefit from stratified storage tanks when used in a closed water heating loop, as the water temperature entering the heat pump is kept at a minimum. Similar observations on the impact of water inlet temperature were made in models developed by White (2002), Stene (2005), and Sarkar *et al.* (2006; 2009). Kim *et al.* (2005) discussed the impact of a SLHX on system level performance of a CO₂ heat pump for water heating. One impact of the SLHX is the increase in superheating of the refrigerant at the compressor suction port. The additional heating and pressure drop through the SLHX resulted in reduced specific volumes at the suction port, and therefore lowered the system mass flow rates. This reduction in mass flow rate would typically lead to reduced component capacities, but the relatively constant compressor work input increases the discharge temperature and enthalpy. The increased discharge

temperature leads to an increase in the driving temperature difference through the gas cooler and effectively offsets the penalty due to the reduced mass flow rate.

Many of the experimental test facilities and simulations that have been used to explore the suitability of CO₂ for water heating applications have been based upon concentric tube-in-tube heat exchangers. While these heat exchangers have a high effectiveness at long lengths, they are generally far from compact at the sizes needed for domestic water heating. Little work has been performed on the use of microchannel-based heat exchangers in these systems, especially for use in hydronically-coupled systems. Microchannel heat exchangers have been shown to reduce heat exchanger size and refrigerant charge of heat pump systems and could aid in the continued successful commercialization of CO₂ water heaters. One additional means of reducing heat exchanger size that has not previously been widely investigated is through repeated recirculation of tank water at a high water flow rate through the gas cooler to meet the desired high water temperature needed for domestic purposes. Much of the prior research used a SLHX in the experimental facilities for cycle testing. Little has been reported on the direct impact of these components, although their use is common. Further research is required to analyze the potential benefit of these components and determine which system operating conditions will benefit the most from their use.

Therefore, this work focuses on extending the previous work on CO₂ heat pump water heaters to include compact microchannel heat exchangers. Two water heating schemes are investigated to analyze the impact on system heat exchanger size and the associated performance tradeoffs. Finally, the performance impacts of a SLHX on the heat pump water heater system are analyzed.

2. SIMPLE SYSTEM MODEL AND COMPONENT DESIGN

Initially, the simplified thermodynamic state model was developed with *Engineering Equation Solver* (EES) (Klein, 2008) to determine the required heat exchanger design conditions at the desired operating condition. With the design conditions fixed, the component models developed in Part I (Goodman *et al.*, 2010) were used to fix the physical dimensions of the heat exchangers, which were then incorporated into the detailed system model described in the following section. Two system configurations were investigated: one with the inclusion of a SLHX and one without. For each configuration, two water heating strategies were investigated: one to heat water to a usable temperature in a single pass through the system and one requiring multiple passes through the system.

The modeled system was coupled to water on the high and low-side through the microchannel gas cooler and evaporator detailed in Part I (Goodman *et al.*, 2010). The gas cooler water loop is assumed to be connected to a storage tank. For the once-through system, the water would be drawn from the tank, heated in one pass to the desired temperature, and returned to the tank. For the multi-pass system, the water would be drawn from the tank, heated to an intermediate temperature, and returned to the tank. The heat pump would continue to operate and draw water from the tank at the intermediate temperature and heat it to progressively higher temperatures until the desired temperature is achieved.

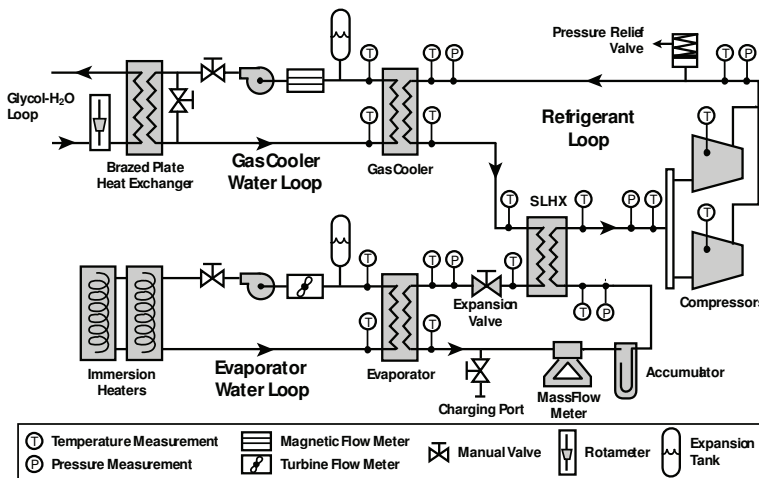


Figure 1: Modeled Heat Pump System with SLHX

2.1 Simplified Model Development

The simplified state point model was developed using design conditions shown in Table 1. By specifying an evaporator closest approach temperature (CAT) and gas cooler approach temperature (ATD), the evaporation saturation and gas cooler outlet conditions are fixed. A fixed superheat was specified, and the compressor isentropic (η_s) and volumetric (η_{vol}) efficiency were determined from the empirical performance models described in Part I. The high-side pressure is an independent variable selected to

Table 1: Nominal Design Conditions

		Water Inlet Temperature [°C]	Water Flow Rate [lpm]	Water Outlet Temperature [°C]
Once-Through	Evaporator	8.3	8.0	-
	Gas Cooler	15	-	60
Multi-Pass	Evaporator	8.3	8.0	-
	Gas Cooler	15	-	35

optimize system COP at the design condition. Fig. 1 shows a schematic of the modeled system, and Fig. 2 shows a pressure-enthalpy diagram of the modeled system with a SLHX. State points 1-7 represent the refrigerant loop, while the remaining state point correspond to the evaporator and gas cooler water inlet and outlet.

For the simplified model, it is assumed that pressure drop through the heat exchangers is negligible and the expansion process between state 7 and 1 is isenthalpic. The saturation condition at state point 1 is found by subtracting the evaporator CAT from the evaporator water outlet temperature (Equation (1)). The quality at state 1 is found from the saturation pressure and assuming the specific enthalpy at state 1 is equal to that of state 7 (SLHX model) or state 6 (non-SLHX model). State point 2 is defined as the saturated vapor state point at T_1 . For the non-SLHX model, state point 3 is a function of the saturation pressure and the superheat temperature only. State point 5 is the isentropic compressor outlet at the desired high-side pressure, with the actual outlet condition (state point 4) found from Equation (2).

$$T_1 = T_{13} - CAT \quad (1)$$

$$i_4 = \frac{i_5 - i_3}{\eta_s} + i_3 \quad (2)$$

The gas cooler exit for both SLHX and non-SLHX models (state 6) is defined by the high-side pressure, and the temperature found by adding the specified ATD to the gas cooler water inlet temperature (state 10). The SLHX couples the gas cooler and evaporator outlet streams together. The compressor inlet temperature (T_3) for the SLHX model is found as shown in Equation (3), where the SLHX effectiveness is assumed constant and the low pressure-side thermal capacitance rate is equal to the minimum of the low and high sides.

$$T_3 = \varepsilon_{slhx} (T_6 - T_2) + T_2 \quad (3)$$

The SLHX heat duty, and high-pressure stream outlet temperature (state 7) can then be found from Equations (4) and (5), where the specific enthalpies are functions of the local pressure and temperature.

$$\dot{Q}_{slhx} = \dot{m}_{ref} (i_6 - i_2) \quad (4)$$

$$i_7 = i_6 - \frac{\dot{Q}_{slhx}}{\dot{m}_{ref}} \quad (5)$$

The refrigerant mass flow rate is calculated by determining the volumetric efficiency from the empirical model proposed in Part I, and Equation (6). The gas cooler and evaporator capacities are then calculated from an energy balance using the calculated mass flow rate and specific enthalpy differences. The maximum possible gas cooler water flow rate is found by performing an energy balance on the calculated gas cooler capacity and the known inlet and outlet water temperatures as indicated in Equation (7). The evaporator water outlet temperature is calculated by performing an energy balance using the evaporator capacity and the specified coolant flow rate and inlet temperature as indicated in Equation (8).

$$\dot{m}_{ref} = \eta_{vol} \cdot V_d \cdot N \cdot \rho_{suc} \quad (6)$$

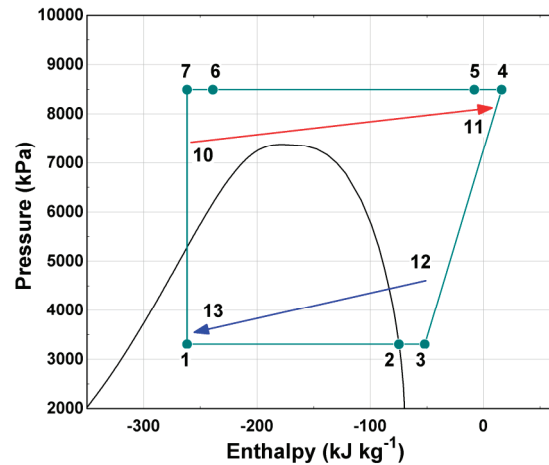


Figure 2: P-h Diagram with SLHX

$$\dot{m}_{water,gc} = \frac{\dot{Q}_{gc}}{i_{11} - i_{10}} \quad (7)$$

$$T_{13} = T_{12} - \frac{\dot{Q}_{evap}}{\dot{m}_{water,evap} \cdot c_{p,avg}} \quad (8)$$

2.2 Simplified Model Results

The results from the simplified model were used to perform detailed sizing of the components for incorporation into the detailed system model. For both the SLHX and non-SLHX systems, parametric studies on the effects of evaporator CAT, gas cooler ATD and SLHX effectiveness on COP were conducted using the nominal design conditions from Table 1. For the non-SLHX system, a 1°C reduction in ATD yielded a 0.8% increase in COP, while a 1°C reduction in CAT yielded a 2.5% increase in COP. Based on the results, an evaporator CAT and gas cooler ATD of 4°C and 2°C were selected to develop both the SLHX and non-SLHX simplified models.

For the non-SLHX system, it was observed that the UA value, a representation of gas cooler size, decreases from 0.454 to 0.298 kW K⁻¹ for the multi-pass system, because the overall gas cooler temperature difference is larger. Likewise, with gas cooler heat duties fixed between the water heating methods, the multi-pass water flow rate was found to be 125% higher than the once-through system. For the SLHX system, the effectiveness of the SLHX was varied from 0.1 to 0.9. Fig. 3 shows the required UA values for the gas cooler and SLHX as a function of SLHX effectiveness. As SLHX effectiveness increases, superheat at the compressor increases; this results in a lower suction density which leads to reduced mass flow rates. The reduction in refrigerant mass flow rate generally reduces the system heating capacity. Counteracting the negative impact of the reduced refrigerant mass flow is a corresponding increase in compressor discharge temperature due to the increased suction temperature. The increased discharge temperature results in larger overall temperature differences between the fluids through the gas cooler and effectively offsets any penalties incurred by the reduced mass flow rate. Thus, gas cooler UA can be seen to decrease with increasing SLHX effectiveness. A SLHX effectiveness of 60% was chosen for the detailed analysis.

For the specified conditions, the required gas cooler UA value for the non-SLHX and SLHX systems are 0.454 and 0.356 kW K⁻¹, respectively, for the once-through system. Similarly, for the multi-pass system, the required gas cooler UA value is 0.298 and 0.256 kW K⁻¹. The SLHX system results in a reduction in gas cooler size of 21.6% and 14.1% for the once-through and multi-pass water heating schemes, respectively. The evaporator UA values are nearly constant for both non-SLHX and SLHX systems at 0.502 and 0.499 kW K⁻¹, respectively. The COPs of the two systems are almost equal, 3.424 and 3.416, respectively. In comparing the results of the two systems, the pressure ratio is approximately equal, 2.53. This results in the compressor power and volumetric efficiency being equal between the systems, since these values are functions of suction and discharge pressures. The superheat at the compressor inlet is increased from 5.0 to 12.3°C resulting in a decrease of the suction density; therefore, the mass flow rate decreases from 0.0180 to 0.0169 kg s⁻¹ between the non-SLHX and SLHX systems. Also, the increase in suction superheat leads to an increase in the compressor discharge temperature from 91.5 to 104.3°C. The decrease in refrigerant mass flow rate is offset by the increase in the compressor discharge temperature, resulting in similar gas cooler heat duties and COP values between the two systems.

2.3 Component Sizing and Design

For a once-through water heating system with no-SLHX, a gas cooler of 20 plates with a water flow rate of 1.26 L min⁻¹ was selected to provide a water delivery temperature of 60°C at the nominal design condition. The same size gas cooler with a different water flow rate was used for systems with a SLHX. For both gas coolers in the once-through scheme, the desired ATD of 2°C could not be reached at the nominal water flow condition, necessitating the reduced flow rates reported. For both SLHX and non-SLHX systems, a gas cooler of 10 plates was used for the multi-pass heating scheme to meet the 2°C ATD design condition and provide 35°C

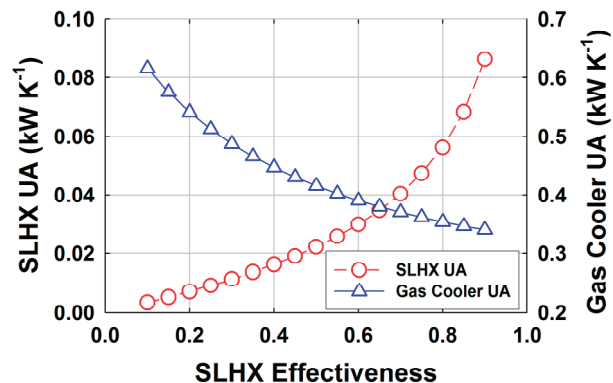


Figure 3: SLHX and Gas Cooler UA vs. SLHX ϵ

water at 3.5 L min^{-1} . From the results of the heat exchanger sizing, the limitations of the near-counterflow gas cooler design compared to true counter flow geometry can be seen. The 2°C ATD requirement could not be satisfied at the once-through low water flow rate. With a higher water flow rate, as in the multi-pass design, the desired heating capacity was easily met with a reasonably sized heat exchanger. The gas cooler design at first appears to be a highly efficient one, given its global counter flow orientation of the water and refrigerant flows, but the heat duty of each water plate and refrigerant pass is still governed by a cross flow fluid orientation that limits the heat exchanger from being able to reach a high effectiveness value. Increasing the water flow rate results in greater temperature differences between the fluids in the heat exchanger and also larger water-side heat transfer coefficients that lead to increased heating capacities. Most other literature that addresses carbon dioxide heat pump water heater performance uses a pure counter flow orientation in the gas cooler, which when sufficiently long can lead to high effectiveness values and eventually low gas cooler ATDs. These designs are usually far from compact. The use of this near-counterflow gas cooler design therefore represents a tradeoff between the benefits of an approximately counter flow design through the use of microchannel geometries, and the excessively large conventional counter flow heat exchangers. It is a significant improvement over a cross flow design; however, this analysis shows that it may be better suited for multi-pass heating rather than for once-through water heating.

The evaporator for the system without a SLHX was sized to meet a heat duty of 3.65 kW while the system with a SLHX needed a heat duty of 3.60 kW. The non-SLHX system required 11 water plates, while the SLHX system required 10 water plates, to meet the desired heat duties. A comparison of the gas cooler and evaporator required for each system configuration is shown in Fig. 4. The SLHX designed with 60% effectiveness at the design conditions required a total length of 0.23 m. The 60% effectiveness value was selected to prevent excessive compressor discharge temperatures.

3. DETAILED SYSTEM MODEL AND RESULTS

The component models developed in Part I of this study with the heat exchanger sizes specified above, were coupled together in an overall system model with linked inputs and outputs between each model.

3.1 Detailed Model Development

The model was solved iteratively in a “loop” around the thermodynamic cycle starting at the compressor and finishing with the evaporator. Inputs from the compressor model allowed solution of the gas cooler subprogram. The gas cooler outputs were then used as inputs for either the evaporator or SLHX. For systems with no SLHX, the gas cooler output, assuming isenthalpic expansion was used as the evaporator inlet. The outlet of the evaporator was checked for convergence by comparing calculated superheat to the specified superheat of 5°C . For the model with a SLHX, the SLHX subprogram was solved using the gas cooler outlet values and the target evaporator outlet condition. The SLHX subprogram output was subsequently used as the input to the evaporator subprogram. After the evaporator output was determined with the evaporator subprogram, the outlet condition was checked for convergence and the evaporator pressure was updated until the desired evaporator outlet condition was met, as discussed below. After evaporator convergence, the updated evaporator pressure was used for the next iteration of the cycle. The entire system model was assumed to have converged when the gas cooler and SLHX heat duties varied by less than 1% on subsequent cycle iterations.

3.2 Detailed Model Results and Discussion

Parametric analyses were performed for both systems (SLHX and non-SLHX) and water heating schemes. The once-through systems were run at evaporator glycol/water inlet temperatures of $-5, 8.3, 25^\circ\text{C}$ and at gas cooler water inlet temperatures of $5, 15, 25,$ and 35°C . The multi-pass systems were run at evaporator water inlet temperatures of $-5.0, 8.3, 25^\circ\text{C}$ and at gas cooler water inlet temperatures of $10, 15, 25, 35,$ and 45°C . It is important to note that the multi-pass system simulations were conducted to determine the performance of the multi-pass system at a specific gas cooler and evaporator water inlet temperature. Later, using this information, the number of recirculations

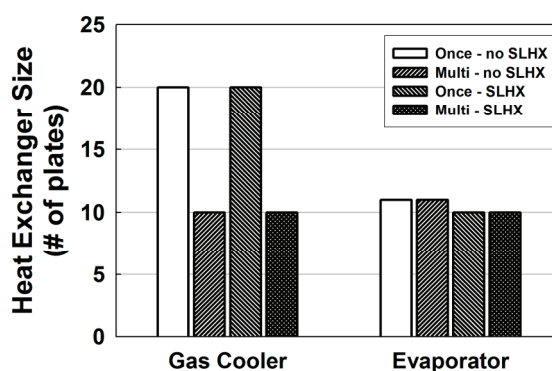


Figure 4: Heat Exchanger Size

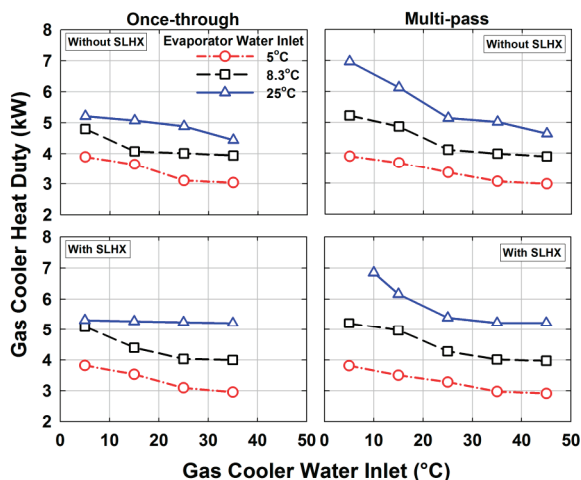


Figure 5: Gas Cooler Heat Duty Results

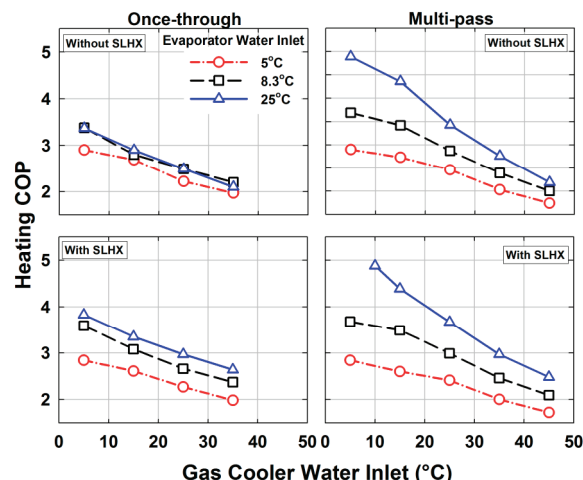


Figure 6: System COP Results

required to meet a target outlet temperature of 60°C and the overall COP value for the process are determined.

The gas cooler heat duties for each system are shown in Fig. 5. At a fixed evaporation pressure, the heat duty decreases with increasing gas cooler water inlet temperature, as the average driving temperature difference decreases and the gas cooler refrigerant outlet temperature is pinched to the gas cooler water inlet. As evaporation pressure increases for a fixed gas cooler water inlet condition, the pressure ratio decreases and refrigerant mass flow rate increases due to an increased compressor suction density and volumetric efficiency. The increase in heat duty at higher evaporator pressure is largest for the multi-pass system. The heat duty is controlled by the overall heat transfer coefficient, or the UA value. The UA of the gas coolers are in turn governed by the largest thermal resistance; a substantial reduction in the lowest thermal resistance will have little effect on the overall heat transfer coefficient. An increase in the refrigerant-side heat transfer coefficient, due to the increased mass flow rate, would not necessarily result in a commensurate increase in the overall heat transfer coefficient if the water-side thermal resistance is already large. Therefore, for the low water flow rate, once-through system, the water-side heat transfer coefficient dominates and the reduction in refrigerant-side thermal resistance due to the increase in refrigerant flow rate as the evaporator pressure increases does not result in a substantial increase in gas cooler heat duty. But for the multi-pass system, the water-side thermal resistance is lower due to the larger water flow rate, so the decrease in refrigerant-side thermal resistance causes a greater increase in heat duty.

As shown in Fig. 6, COP values varied from 2.0 to 3.7 for the once-through system and 1.8 to 4.8 with the multi-pass system over a range of gas cooler and evaporator inlet water conditions. In general, at higher evaporation temperatures, gas cooler heat duty increases while compressor pressure ratio and work input are reduced, resulting in higher COP values. Fig. 7 summarizes the relative change in COP caused by the inclusion of a SLHX compared to a system without the SLHX at the same conditions. As the gas cooler water inlet temperature increases, the relative benefit of the SLHX on heating COP tends to increase. At the highest evaporation pressure, the benefit of the SLHX approached 25% for the once-through system and 15% for the multi-pass system. However, at the lowest evaporation pressure, the COP is reduced by up to 5%. The reduction in COP at low evaporation temperature may be attributed to the reduced refrigerant mass flow rate due to the increased suction specific volume resulting from the inclusion of the SLHX. At the lowest evaporation temperature, the pressure ratio is the highest, and the mass flow lowest. Thus, as the UA of the gas cooler under consideration is dominated by the refrigerant thermal resistance (Fronk and Garimella, 2009), a further reduction in refrigerant mass flow rate and the corresponding heat duty has a negative effect on COP. At the higher evaporation conditions, the gas cooler heat duty is less sensitive to the reduction in mass flow rate and COP is observed to increase due to the higher

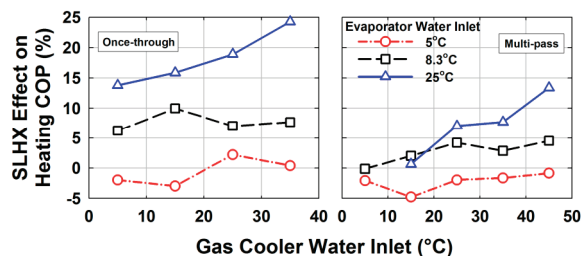


Figure 7: SLHX effect on COP

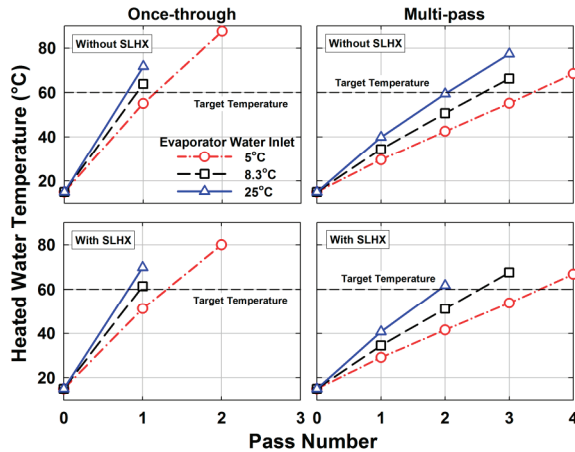


Figure 8: Water Temperature vs. Pass Number

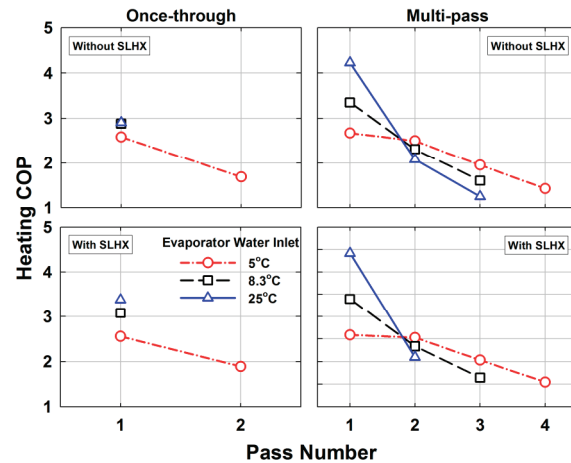


Figure 9: System COP vs. Pass Number

discharge temperature and resulting driving temperature difference.

4 COMPARISON OF WATER HEATING SCHEMES

The COPs reported in Fig. 6 are for a fixed gas cooler water inlet. For the once-through water heating system this is a good approximation of real system operation. However, for a multi-pass system the water inlet temperature and associated COP change with time. Thus, a method for estimating the overall COP of the multi-pass system using the results of the detailed system model at a set of conditions is necessary. To provide an equal comparison between the systems, a 200 L water tank was assumed to be connected to each heat pump. The heat pump drew water from the bottom of the tank, heated it, and returned it to the top of the tank. For heat pump systems that require multiple passes to heat the water to the desired 60°C water temperature, the tank water is assumed to be stratified. Also, for these systems, the transient response and thermal mass of the heat pump and associated plumbing is ignored.

From the detailed simulation results above, models were developed to predict COP and gas cooler water outlet temperature as a function of evaporator and gas cooler water inlet temperatures for the four system combinations. The resulting models were in the form of a biquadratic equation shown in Equation (9), where each system type and water heating scheme combination had a unique set of coefficients.

$$z = a_1 + a_2 T_{gc,water,in} + a_3 T_{gc,water,in}^2 + a_4 T_{evap,water,in} + a_5 T_{evap,water,in}^2 + a_6 T_{gc,water,in} T_{evap,water,in} \quad (9)$$

This set of equations is used to calculate discharge temperature and COP value for each water pass, where the resulting gas cooler outlet temperature is used as the inlet temperature of the subsequent pass, with the process continuing until the desired outlet of 60°C is achieved. Figs. 8 and 9 show the resulting gas cooler water outlet temperature and system COP for each water pass, respectively. Up to four water passes are needed for the multi-pass system to bring the tank water temperature above the desired temperature of 60°C. It should be noted that even with the larger system designed to heat the water in a single pass, the -5°C evaporator temperature case will require additional water heating past that provided by the first pass to meet the desired temperature.

As seen in Fig. 8, the discharge temperature for the final passes of many of the systems is greater than 60°C. Therefore, the final pass for each system will only require a fraction of the total tank volume to meet the desired overall tank temperature. To provide a valid comparison between all of the systems, the total energy required to bring the tank from an initial temperature of 15 to 60°C for a 200 L tank volume was found to be 37.31 MJ. The energy delivered to the tank in each pass through the heat pump is defined in Equation(10).

$$Q_{pass,j} = \left(\frac{V_{pass,j}}{V_{water}} \right) \dot{m}_{water} (i_{j,out} - i_{j,in}) \quad (10)$$

In the above equation, j represents the pass number, and $i_{j,out}$ and $i_{j,in}$ represent the outlet and inlet enthalpy of the heat pump calculated at the outlet and inlet water temperature of the pass of interest. The volume of water circulated through the heat pump in the pass of interest is represented by $V_{pass,j}$, which is 200 L for all but the final pass. The total electrical energy required to deliver the required tank energy is defined by Equation (11) where COP_j is the COP of the pass of interest and k is the total number of passes required. The overall COP is then calculated using Equation (12). The results of the overall COP calculations for each system combination are shown in Fig. 10.

$$W_{hp} = \sum_{j=1}^k \frac{Q_{pass,j}}{COP_j} \quad (11)$$

$$COP_{overall} = \frac{Q_{tank}}{W_{hp}} \quad (12)$$

The values in Fig. 10 represent the COP that would be expected for each of the four heat pumps to heat a tank of water from 15 to 60°C. The COP variation across the evaporator temperatures of -5 to 25°C were 2.45 to 2.90 for the once-through system without a SLHX, 2.20 to 2.89 for the multi-pass system without a SLHX, 2.40 to 3.38 for the once-through system with SLHX, and 2.21 to 3.00 for the multi-pass system with SLHX. For all temperatures, the once-through systems outperform the multi-pass systems. The once-through, no-SLHX system outperforms the multi-pass, no-SLHX by an average of 10% across the three evaporator temperatures. The once-through, SLHX system outperforms the multi-pass, SLHX system by an average of 15%. However, the required gas cooler size for the once-through system was twice that required for the multi-pass system. The use of the SLHX for the low evaporator temperature of -5°C reduced the performance of the once-through system by 2.1% and only increased the multi-pass performance by 0.4%. More benefit from the SLHX is seen at higher evaporator temperatures. An increase in COP of 7.0% for the once-through and 2.1% for the multi-pass system is seen at an evaporation temperature of 8.3°C and 16.5% and 4.1% for the once-through and multi-pass systems at 25°C.

At low evaporator temperatures, the reduction in refrigerant mass flow rate due to the increase in compressor suction specific volume caused by the SLHX adversely affects performance more than the performance improvement due to the increased compressor outlet temperature. The SLHX is most effective for the once-through systems where the temperature differences between the fluids in the gas cooler are small due to the high temperature lift of the water for these systems. Increased temperature differences play an important role in the once-through systems, whereas for the multi-pass systems, the temperature differences are already higher due to the higher water flow rate.

5. CONCLUSIONS

Analytical models of microchannel based heat exchangers and an empirical model of a reciprocating compressor developed and validated with experiments in Part I (Goodman *et al.*, 2010) of this study were used to design a residential water heating system and develop a detailed system level model. Investigations on two system configurations, with and without a SLHX, and two water heating schemes, once-through and multi-pass were conducted. Results from a simplified thermodynamic state point model were used to define the design conditions for each heat exchanger, which were then sized using the previously developed component models and incorporated into a detailed system model. The gas cooler for the once-through system had 20 water plates; while for the multi-pass system, the gas cooler had 10 plates. The evaporator of the no-SLHX system had 11 plates, while the evaporator of the SLHX system had 10 plates. The SLHX length was determined to be 0.23 m to meet the required 60% effectiveness.

The detailed system model calculated gas cooler COP and water outlet temperature at a single instant under varying conditions for each water heating scheme and

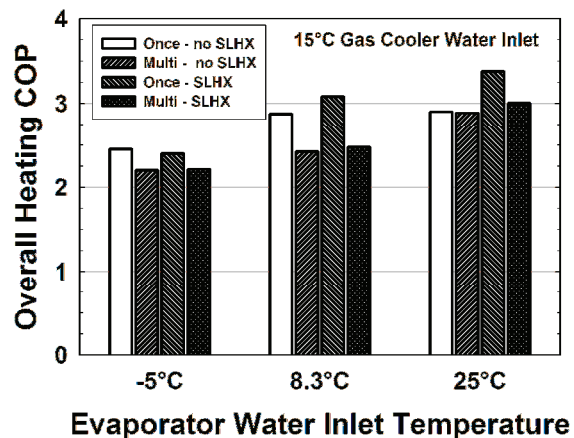


Figure 10: Overall Heating COP

system configuration. The effect of the SLHX on system COP was analyzed and shown to be detrimental to performance at the -5°C evaporator temperature, with penalties of nearly 5%. At an evaporator temperature of 25°C , the SLHX benefited the once-through system by nearly 25% for the 35°C gas cooler water inlet case. The multi-pass system also indicated an improvement with the use of the SLHX, with the 25°C evaporator and 45°C gas cooler inlet temperature case showing a 14% improvement in COP. Finally, an approach was developed to simulate heating a tank of water from 15 to 60°C using the instantaneous results of the detailed model. The multi-pass system required 2 to 4 water recirculations to provide the desired level of heating. The once-through, no-SLHX system outperformed the multi-pass, no-SLHX system by an average of 10.2% when a 15°C tank of water was raised to 60°C . For the SLHX systems, the once-through system outperformed the multi-pass by 15.2%. To obtain these higher performance values, a gas cooler that was twice the size of the gas cooler for the multi-pass system was needed.

While this study has provided insight into the benefits and tradeoffs of using a SLHX and two heating schemes, additional work can be performed to further improve the accuracy of the model or investigate different options to increase performance. The detailed model utilizes a fixed superheat and optimal pressure based on each operating condition. This implies either a varying system charge, or a method of varying system volume to control superheat and high-side pressure. Developing a model that predicts how superheat and high-side pressure change with a fixed system refrigerant charge from the design point as evaporator and gas cooler inlet conditions change would yield a more accurate comparison between the two systems and water heating strategies. Additionally, considering other advanced components such as scroll compressors or ejectors may be warranted to investigate potential system performance increases.

NOMENCLATURE

a	constant coefficient	(-)	Subscripts	
c_p	specific heat	($\text{kJ kg}^{-1} \text{ }^{\circ}\text{C}^{-1}$)	d	displacement
ε	effectiveness	(-)	dis	discharge
η	efficiency	(-)	evap	evaporator
i	specific enthalpy	(kJ kg^{-1})	gc	gas cooler
\dot{m}	mass flow rate	(kg s^{-1})	hp	heat pump
N	compressor speed	(rad s^{-1})	j	index notation
P	pressure	(kPa)	ref	refrigerant
\dot{Q}	heat duty	(kW)	s	isentropic
Q	total heat	(kJ)	suc	suction
ρ	density	(kg m^{-3})	vol	volumetric
T	temperature	($^{\circ}\text{C}$)		
V	volume	(m^3)		
\dot{V}	volumetric flow rate	($\text{m}^3 \text{ s}^{-1}$)		
W	total work	(kJ)		

REFERENCES

- Cecchinato, L., M. Corradi, E. Fornasieri and L. Zamboni (2005), "Carbon Dioxide as Refrigerant for Tap Water Heat Pumps: A Comparison with the Traditional Solution," *International Journal of Refrigeration* Vol. 28(8) pp. 1250-1258.
- Fronk, B. and S. Garimella (2009). *Modeling and Testing of Water-Coupled Microchannel Gas Coolers for Natural Refrigerant Heat Pumps*. 3rd IIR Conference on Thermophysical Properties and Transfer Processes of Refrigerants. Boulder, CO, International Institute of Refrigeration.
- Goodman, C., B. Fronk and S. Garimella (2010), "Transcritical Carbon Dioxide Microchannel Heat Pump Water Heaters: Part I - Validated Component Simulation Modules," *13th International Refrigeration and Air Conditioning Conference*, West Lafayette, IN
- Kim, M.-H., J. Pettersen and C. W. Bullard (2004), "Fundamental Process and System Design Issues in CO_2 Vapor Compression Systems," *Progress in Energy and Combustion Science* Vol. 30(2) pp. 119-174.

- Kim, S. G., Y. J. Kim, G. Lee and M. S. Kim (2005), "The Performance of a Transcritical CO₂ Cycle with an Internal Heat Exchanger for Hot Water Heating," *International Journal of Refrigeration* Vol. 28(7) pp. 1064-1072.
- Klein, S. A. (2008). *Engineering Equation Solver*, F-Chart Software.
- Neksa, P., H. Reksad, G. R. Zakeri and P. A. Schiefloe (1998), "CO₂-Heat Pump Water Heater: Characteristics, System Design and Experimental Results," *International Journal of Refrigeration* Vol. 21(3) pp. 172-179.
- Rigola, J., G. Raush, C. D. Perez-Segarra and A. Oliva (2005), "Numerical Simulation and Experimental Validation of Vapour Compression Refrigeration Systems. Special Emphasis on Co²," *International Journal of Refrigeration* Vol. 28(8) pp. 1225-1237.
- Sarkar, J., S. Bhattacharyya and M. R. Gopal (2006), "Simulation of a Transcritical CO₂ Heat Pump Cycle for Simultaneous Cooling and Heating Applications," *International Journal of Refrigeration* Vol. 29(5) pp. 735-743.
- Sarkar, J., S. Bhattacharyya and M. Ramgopal (2009), "A Transcritical CO₂ Heat Pump for Simultaneous Water Cooling and Heating: Test Results and Model Validation," *International Journal of Energy Research* Vol. 33(1) pp. 100-109.
- Stene, J. (2005), "Residential CO₂ Heat Pump System for Combined Space Heating and Hot Water Heating," *International Journal of Refrigeration* Vol. 28(8) pp. 1259-1265.
- White, S. D., M. G. Yarrall, D. J. Cleland and R. A. Hedley (2002), "Modelling the Performance of a Transcritical CO₂ Heat Pump for High Temperature Heating," *International Journal of Refrigeration* Vol. 25(4) pp. 479-486.

ACKNOWLEDGEMENTS

Financial support from the US Army Ft. BelVoir office through a subcontract from Modine Manufacturing Company is gratefully acknowledged. The authors also thank Modine Manufacturing Company for supplying several of the test heat exchangers and associated components. Assistance from, and insightful discussions with Mr. John Manzione, Dr. Stephen B. Memory, Mr. David Garski, Mr. Sam Collier, and Mr. Mark Hoehne for conducting this research are also acknowledged.